Environ Earth Sci
DOI 10.1007/s12665-011-1144-3

ORIGINAL ARTICLE

Integrating hydrologic modeling and land use projections for evaluation of hydrologic response and regional water supply impacts in semi-arid environments

Minxue He · Terri S. Hogue

Received: 2 September 2010 / Accepted: 6 June 2011

Abstract Semi-arid environments are generally more sensitive to urbanization than humid regions in terms of both hydrologic modifications and water resources sustainability. The current study integrates hydrologic modeling and land use projections to predict long-term impacts of urbanization on hydrologic behavior and water supply in semi-arid regions. The study focuses on the Upper Santa Clara River basin in northern Los Angeles County, CA, USA, which is undergoing rapid and extensive development. The semi-distributed Hydrologic Simulation Program Fortran (HSPF) model is parameterized with land use, soil, and channel characteristics of the study watershed. Model parameters related to hydrologic processes are calibrated at the daily time step using various spatial configurations of precipitation and parameters. Potential urbanization scenarios are generated on the basis of a regional development plan. The calibrated (and validated) model is run under the proposed development scenarios for a 10 year period. Results reveal that increasing development increases total annual runoff and wet season flows, while decreases are observed in existing baseflow and groundwater recharge during both dry and wet seasons. As development increases, medium-sized storms increase in both peak flow and overall volume, while low and high flow events (extremes) appear less affected. Urbanization is also shown to decrease natural recharge and, when considered at the regional scale, may result in a loss of critical water supply to Southern California. The current study provides a coupled framework for a decision support tool that can guide efforts involved in regional urban development planning and water supply management.

Keywords Urbanization · Watershed · Hydrology · Water supply · HSPF · California

Introduction

Throughout Southern California, large areas of native land cover are disappearing due to rapid and extensive urbanization. The transformation from native to developed lands results in the addition of impervious material (concrete, asphalt, etc.), conveyance (culverts, channels, pipes) as well as detention systems, and transition from native to non-native vegetation species (grass, palms, woody plants, etc.). These conversions typically result in hydromodification of stream systems, increasing wet weather runoff and shifting the timing and volume of flood peaks (Murdock et al. 2004; Wissmar et al. 2004; White and Greer 2006; Vicars-Groening and Williams 2007; Beighley et al. 2008; Andriani and Walsh 2009; Im et al. 2009; Quan et al. 2010). Increased flow rates typically lead to extensive channel erosion and instability (Bledsoe and Watson 2001; Miller and Kochel 2010). In addition, the compaction of soils and addition of paved surfaces reduces infiltration, alters channel baseflow, and, more importantly, may reduce long-term recharge to regional aquifers (Finkenbine et al. 2000; Toran et al. 2009; Pandey et al. 2010).

M. He · T. S. Hogue
Department of Civil and Environmental Engineering,
University of California, Los Angeles, CA, USA

Present Address:
M. He (✉)
Office of Hydrologic Development,
NOAA National Weather Service, Silver Spring, MD, USA
e-mail: minxuehe@gmail.com

M. He
Riverside Technology, Inc., Fort Collins, CO, USA

Published online: 22 June 2011

Urbanization-related changes in stream discharge, infiltration, baseflow patterns, and groundwater recharge can significantly impact regional water availability. Along with expanding urbanization, population and water demand are dramatically increasing in many semi-arid regions, including Southern California. The combination of spreading urbanization and increasing population make historically dependable water supplies suspect in Southern California, which relies heavily on recharged groundwater and imported water (MWD 2005). In this regard, it is of vital importance to predict the potential impact of expanding urbanization on hydrologic processes (baseflow, recharge, infiltration rates) and the specific fluxes critical to regional water supply in semi-arid environments.

In general, most development impacts are described on an event-specific basis (Bhaduri et al. 2000; Konrad et al. 2005). Relatively few studies (Bhaduri et al. 2000) characterize long-term (e.g., seasonal or annual) alterations in the hydrologic response of urbanized watersheds. McClintock et al. (1995) argued that the long-term impacts of urbanization on water quantity are dominantly controlled by the cumulative effects of minor storm events instead of high-magnitude storm events. Bhaduri et al. (2000) successfully applied the long-term hydrologic impact assessment (L-THIA) model to address the long-term hydrologic impacts of urbanization. However, limited by the simple structure of the model, Bhaduri et al. (2000) only provided an initial assessment of hydrologic impacts focusing on the response of annual average runoff.

Numerous models have been employed for continuous simulations of basin streamflow, including the US Environmental Protection Agency's Hydrologic Simulation Program Fortran (HSPF) model, a semi-distributed hydrologic model that continuously simulates surface and subsurface flow as well as water quality processes (Bicknell et al. 2001). The model has been extensively applied in various practices, including simulation of streamflow (Brun and Band 2000; Bledsoe and Watson 2001; Hayashi et al. 2004; Kim et al. 2007; Choi and Deal 2008; Chung and Lee 2009), baseflow (Brun and Band 2000), streamflow temperature (Chen et al. 1998a, b), as well as stream loadings of nutrients, pesticide, and sediments from agricultural and urbanizing watersheds (Tong and Chen 2002; El-Kaddah and Carey 2004; Hayashi et al. 2004; Keller et al. 2004; Luo et al. 2007; Marcé and Armengol 2009). The size of the watersheds studied in these applications ranges from 14.7 km^2 (Des Moines Creek Watershed, Washington, US; Bledsoe and Watson 2001) to 1,000,000 km^2 (Upper Yangtze River Basin, China; Hayashi et al. 2004), indicating the applicability of the HSPF to both small and large watershed systems.

Limited studies (Brun and Band 2000; Bledsoe and Watson 2001; Choi and Deal 2008) have demonstrated the capabilities of the HSPF model in simulating urbanization-related changes in discharge. However, none of these studies focused on arid or semi-arid urban regions. Compared to humid regions, arid and semi-arid watersheds provide unique modeling challenges (Keller et al. 2004; Ackerman et al. 2005). During storm events, flow in arid watersheds is extremely flashy (Tiefenthaler et al. 2001). In the dry season, natural flows can decrease significantly and baseflow may be intermittent. Many arid regions also depend on imported water, which is difficult to account for in water budget studies or model simulations (Ackerman et al. 2005). In addition, limited studies have noted that arid environments may be more sensitive to urbanization than humid regions (Caraco 2000; Ourso and Frenzel 2003). Lack of both hydrological and chemical data has limited rigorous evaluation and implementation of water quality models (e.g., SWAT, HSPF, WARMF) in semi-arid regions. Consequently, this has limited their reliability as predictive tools for establishment of total maximum daily loads (TMDLs) or future development scenarios on urbanizing watersheds. Ackerman et al. (2005) evaluated the performance of the HSPF model on two semi-arid watersheds (one urban and one largely undeveloped) in Southern California at three time scales: hourly, daily, and annual. The model performed fairly well at the daily and longer time scales, but problems were noted at shorter model time scales and dry season simulations (especially in the more urbanized system). Poor representation of rainfall spatial variability and dry weather flows from urban runoff (imported water) were key issues in degradation of model performance (Ackerman et al. 2005).

The current study undertakes an assessment of future land cover change in the Santa Clara River basin in northern Los Angeles County, home to a commuter population for the City of Los Angeles and undergoing rapid and extensive development. To evaluate the impacts of expanding urbanization on overall hydrologic behavior and regional water supply, we address the following objectives: (1) assess the applicability of a spatially distributed HSPF model (configured with distributed model input and parameters) in semi-arid watersheds, (2) predict changes in the hydrologic response (surface flow, infiltration, baseflow, etc.) to varying levels of projected urbanization, and (3) quantify the potential loss of subsurface water supply (recharge) given extensive basin development. Urbanization scenarios for future expansion are established based on regional development plans. The hydrologic response from the development scenarios is compared to calibrated, baseline simulations, and relative changes in various flow regimes are investigated. The implications of the study in guiding urban development planning and regional water supply management are also discussed.

Study area

The current study focuses on the Upper Santa Clara River watershed (USCRW) located approximately 50 km north of the City of Los Angeles, California (Fig. 1). The 1,680 km^2 USCRW consists primarily of natural vegetation (chaparral and grassland), with concentrated urban and residential lands in the Santa Clarita Valley (SCV) right above the outlet of the watershed. The watershed has an average slope of 3.4%, with elevation ranging from 243 to 2,014 m. The climate is semi-arid with an average annual precipitation of 461 mm and mean temperature of 25°C in summer and 9°C in winter. The majority of the annual precipitation occurs between November and April.

Primary land cover in undeveloped areas in the USCRW is chaparral, which collectively accounts for 70% of the total basin area. Grassland accounts for 17% of the basin area. Urbanized land cover, located mostly in the SCV, accounts for about 10% of the basin area. Soils in the watershed are fairly porous and include higher percentages of sandy (sand/loamy sand/sandy loam; 42%) and loamy soils (loam/silty loam; 43%) and smaller amounts of clayey soils (loam/silty clay; 15%). There are two water reclamation plants (WRP), Valencia WRP and Saugus WRP within SCV, which discharge directly to the main stream of the Santa Clara River. Castaic Lake, a water supply reservoir for the California aqueduct, is located in the northwest corner of the study area.

Methods

Modeling framework

HSPF is a conceptual, watershed-scale model, which simulates channel discharge as well as various water quality constituents. Use of HSPF requires division of the watershed into land segments (based on land cover) and river reaches. Each land segment is referred to as a hydrologic response unit (HRU). Partitioning of surface runoff/infiltration is governed by Philips equation (Philips 1957). Runoff then moves laterally to downslope segments or to a river reach or reservoir. Other simulated processes include interception, percolation, interflow, and groundwater movement. The HSPF applies Manning's equation for routing overland flow and kinematic wave method for channel routing. In the current study, an hourly timestep

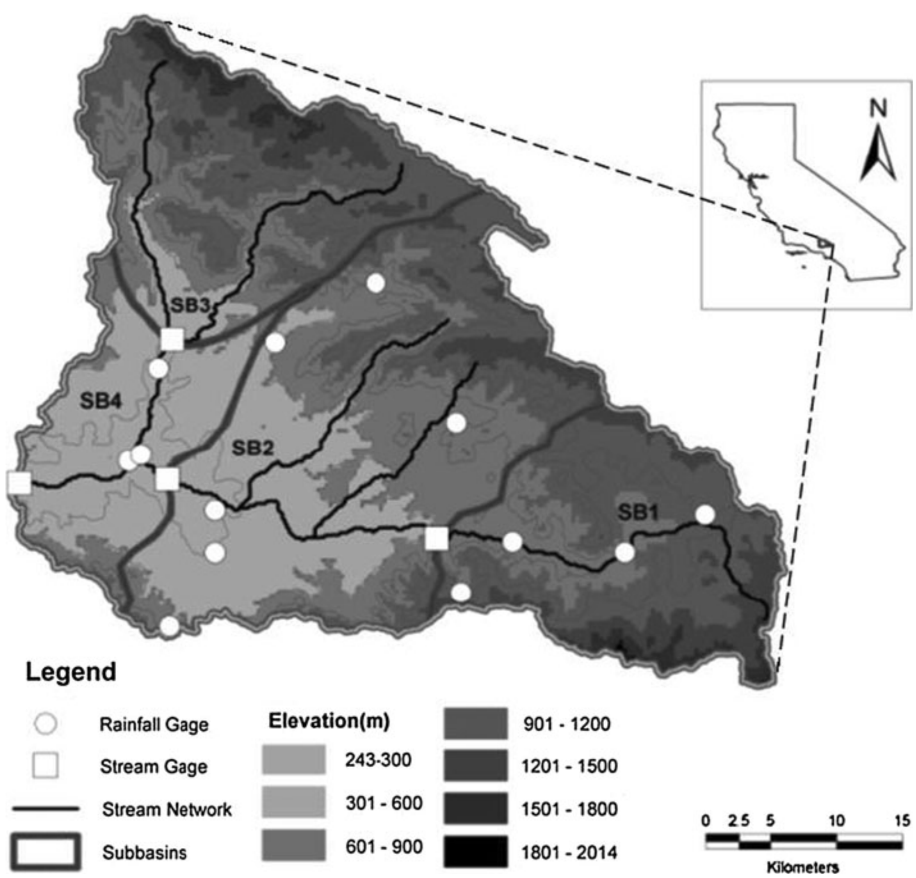

Fig. 1 Upper Santa Clara River Watershed (USCRW) located in northern Los Angeles County, including shaded elevation bands. Precipitation gages (*circles*) and stream gages (*squares*) are shown, as well as channel network (*dark lines*) and sub-basin designations (SB1–SB4)

was used as the computational interval for model simulations; output was aggregated to the daily timestep for evaluation and comparison since observed streamflow was only available at the daily scale. The model consists of three modules, PERLND, IMPLND, and RCHRES, which simulate the hydrologic and water quality processes over pervious land segments, impervious land segments, and through free-flowing reaches and well-mixed lakes, respectively. For this study, only the hydrologic processes were simulated using the HSPF (water quantity). The HSPF model requires rainfall, potential evapotranspiration, land use, and channel geometry as inputs.

The USCRW outlet and model simulation point is the US Geological Survey (USGS) stream gage #11109000. Above this point, the watershed was delineated into four sub-basins (Fig. 1). Sub-basin one consists of 401 km^2 of mostly natural land with 3% developed area. The SCV is located across the boundary of sub-basins two (685 km^2) and four (217 km^2). Approximately 18% of these two sub-basins are developed. The Newhall Ranch, which is the main region undergoing significant urbanization in the SCV, is located within sub-basin four. The Saugus WRP is in sub-basin two and was put into operation in 1962. The Valencia WRP is in sub-basin four and started operation in 1967. Castaic Lake forms most of sub-basin three (outlet USGS stream gage #11108134). The Castaic Lake outflow is formulated as a point source within the HSPF model, releasing flow to sub-basin four. Incorporation of Castaic Lake and the two WRPs into the simulation requires the corresponding flow discharge data from the lake and WRPs. Calibration and validation of the model requires observed streamflow at the outlet.

Data collection

Daily rainfall data were obtained from 13 rainfall gages [water years (WY) 1966–2006] maintained by the Los Angeles Department of Power and Water (LADPW) within the study watershed (Fig. 1). Some gages contained occasional missing data. Rainfall data from nearby gages were used to extrapolate missing data based on the inverse-distance method. Daily data were uniformly disaggregated to an hourly timestep to use as input for the HSPF model. To facilitate continuous modeling, the Thiessen Polygon method was utilized to create a mean areal rainfall time series for the relevant study areas (determined during initial calibration and model discretization). Hourly reference (potential) evapotranspiration (ETo) data were obtained from the California Irrigation Management Information System (CIMIS) Station #101 (WY 1992–2006). Actual evapotranspiration is computed internally in the HSPF based on the input reference evapotranspiration data and model parameters.

Channel networks and cross sections were produced through the US Environmental Protection Agency (USEPA) software Better Assessment Science Integrating Point and Non-point Sources (BASINS) (USEPA 2004) using the BASINS Digital Elevation Model (DEM) data and National Hydrography Dataset (NHD). Outflow data from the USCRW outlet and Castaic Lake storage facility (sub-basin three outlet) was obtained from the USGS (WY 1966 to 2006). Discharge data from the two WRPs were available from WY 1975 to 2006 and obtained from the Sanitation Districts of Los Angeles County. A 2000-land cover data set was obtained from the National Oceanic and Atmospheric Administration (NOAA) Coastal Services Center (NOAA-CSC 2003). This LANDSAT-based data product was used to define the model land segments and calibrate the HSPF model. The 30 m resolution data contains 39 land use categories, which are aggregated into eight land use types based on a similarity analysis (NOAA-CSC 2003). The imperviousness of each aggregated land use was determined using the Los Angeles Department of Power and Water guidelines (DePoto et al. 1991). The aggregated land use categories and corresponding imperviousness for the entire study area are presented in Table 1.

Model calibration and validation

The model simulation period (WY 1997–2006) was selected based on the availability of precipitation, reference evapotranspiration, and discharge data. The data period was split to allow a split-sample analysis of model performance (Refsgaard and Knudsen 1996): 1999–2002 were used for model calibration and 2003–2006 were used for independent model evaluation (validation). The 1997–1998 period was used as an initialization (spin-up) period. Calibration was conducted by manually adjusting model parameters to achieve agreement between simulated and observed flows for the outlet location using visual inspection and multiple statistical criteria. Four calibration scenarios with varying lumped and distributed precipitation

Table 1 Upper Santa Clara River Watershed (USCRW) land use (as % of area) and estimated imperviousness for each aggregated land use

Aggregated land use	% Area	% Imperviousness
Commercial/industrial	0.78	90
High residential	1.34	60
Low residential	1.45	40
Rural residential	6.81	20
Chaparral	88.70	6
Open ground	0.12	3
Water and wetlands	0.80	0

Impervious estimates derived from Los Angeles Department of Water and Power (LADWP) (DePoto et al. 1991) input and model parameters were evaluated to determine the most suitable model configuration. A lumped configuration represents a single value (model parameter or input) applied to the three modeled sub-basins (one, two and four), while a distributed configuration means different values are applied to each of the three sub-basins (precipitation inputs and parameter values are specific to each sub-basin). Specifically, for the four scenarios (C1–C4): C1 consists of lumped (same values for all basins) inputs and lumped (same values for all basins) parameters; C2 consists of lumped inputs and distributed parameters (sub-basin specific parameters); C3 consists of distributed precipitation inputs (sub-basin specific precipitation inputs) and lumped parameters; C4 consists of distributed precipitation inputs and distributed parameters.

Results from the various calibration scenarios were evaluated using criteria proposed by Donigian (2002), including bias (BIAS), correlation (R), standard deviation ratio (RSR), and Nash–Sutcliffe efficiency (NSE). Once a calibration scenario is selected and parameters finalized, testing of the calibrated model is undertaken during the validation period. Specific formulations for the evaluation statistics are given as:

$$\mathrm{BIAS} = \frac{\sum_{i=1}^{n} \left(Q_i^{\mathrm{obs}} - Q_i^{\mathrm{sim}}\right)}{\sum_{i=1}^{n} Q_i^{\mathrm{obs}}} \times 100 \quad (1)$$

$$R = \frac{\sum_{i=1}^{n} \left(Q_i^{\mathrm{obs}} - Q_{\mathrm{obs}}^{\mathrm{mean}}\right)\left(Q_i^{\mathrm{sim}} - Q_{\mathrm{sim}}^{\mathrm{mean}}\right)}{\sqrt{\sum_{i=1}^{n} \left(Q_i^{\mathrm{obs}} - Q_{\mathrm{obs}}^{\mathrm{mean}}\right)^2 \left(Q_i^{\mathrm{sim}} - Q_{\mathrm{sim}}^{\mathrm{mean}}\right)^2}} \quad (2)$$

$$\mathrm{RSR} = \frac{\mathrm{RMSE}}{\mathrm{STDEV_{obs}}} = \frac{\sqrt{\sum_{i=1}^{n} \left(Q_i^{\mathrm{obs}} - Q_i^{\mathrm{sim}}\right)^2}}{\sqrt{\sum_{i=1}^{n} \left(Q_i^{\mathrm{obs}} - Q_{\mathrm{obs}}^{\mathrm{mean}}\right)^2}} \quad (3)$$

$$\mathrm{NSE} = 1 - \frac{\sum_{i=1}^{n} \left(Q_i^{\mathrm{obs}} - Q_i^{\mathrm{sim}}\right)^2}{\sum_{i=1}^{n} \left(Q_i^{\mathrm{obs}} - Q_{\mathrm{obs}}^{\mathrm{mean}}\right)^2} \quad (4)$$

where, Q^{obs} and Q^{sim} are observed and simulated flows, respectively; $Q_{\mathrm{obs}}^{\mathrm{mean}}$ and $Q_{\mathrm{sim}}^{\mathrm{mean}}$ are the mean value of observed flows and simulated flows, respectively; RMSE is the root mean squared error; $\mathrm{STDEV_{obs}}$ is the standard deviation of observed flows. Statistics were calculated for the calibration and validation periods at the annual, monthly, and daily time scales, as well as for the wet season (1 October–31 May) and dry season (1 June–30 September) at the daily time scale.

Scenario modeling

A second land cover data set was generated from information obtained from the Newhall Ranch Development Plan (Newhall Land 1999). According to the Newhall Plan, approximately 23 km^2 will be developed in 25 years within the Newhall Ranch area located in sub-basin four. The proposed land cover types in the Newhall Plan were aggregated into four categories (commercial/industrial, high residential, low residential, and rural residential). The corresponding areas of each of the four categories (and corresponding impervious) were estimated (Table 2). The initial proposed development pattern (current plan) is hereafter referred to as Scenario 1 (S1). Based on S1, three other development scenarios are created to simulate future development, which may occur over the long term in the study watershed. Specifically, Scenario 2 (S2) doubles the development areas of S1. Scenario 3 (S3) doubles S2 and Scenario 4 (S4) triples S2 (Table 2). Several of these scenarios (S3 and S4) may currently be somewhat unrealistic given the potential constraints on the system (transportation, water demand, etc.). However, these high-density cases were formulated to assess the impacts of extreme urbanization on regional water fluxes in the USCRW (and potentially other semi-arid basins undergoing development).

The validated model is run under the proposed development scenarios to simulate flows for the entire watershed for the period WY 1997–2006. Model simulations from sub-basin four are then analyzed to evaluate future urbanization in this region of the watershed. Predictions of total runoff for the various scenarios are compared to the baseline simulation obtained from the current land cover scenario at a range of time scales: daily, seasonal (dry and wet), and annual. The influence of urban development on storm events with varying magnitude is also investigated. The ten largest storm events (based on volume) are selected for each year during the simulation period (100 total storms). Flow duration curves are constructed for baseline and land cover changes scenarios for the selected storms. Changes in peak flow and total storm volume are also analyzed for developed scenarios. In addition, investigation of the influence of urbanization on specific flow components including baseflow, surface (overland and lateral) flow, and recharge to the groundwater system is evaluated for each of the four proposed scenarios. The HSPF model uses the parameter DEEPFR to estimate the fraction of infiltrating water recharged to deep groundwater; the remaining portion (i.e., 1-DEEPFR) provides baseflow to the stream (Duda et al. 2001). Both baseflow and recharge fluxes are calculated based on DEEPFR. Surface flow is obtained by subtracting the baseflow from the total flow simulated.

Results

Data analysis

Long-term precipitation for the study period (WY 1966–2006) was estimated at 423 mm. A simple assessment of

Table 2 Current and proposed land use scenarios for sub-basin four: scenario one (S1) is derived using regional development plans, scenario two (S2) is double the development area of S1, scenario three (S3) is double the development area of S2 and scenario four (S4) is triple the development area of S2

Land use type	Current area (km^2)	S1 (km^2)		S2 (km^2)	
		Proposed	Aggregated	Proposed	Aggregated
Commercial/industrial	2.13	2.30	4.43	4.60	6.73
High residential	1.85	11.52	13.37	23.04	24.89
Low residential	2.17	6.91	9.08	13.82	15.99
Rural residential	33.41	2.30	35.71	4.60	38.01
Total	39.56	23.03	62.59	46.06	85.62
Fraction of sub-basin four (%)	18.23		28.84		39.46
Land use type	Current area (km^2)	S3 (km^2)		S4 (km^2)	
		Proposed	Aggregated	Proposed	Aggregated
Commercial/industrial	2.13	9.20	11.33	13.80	15.93
High residential	1.85	46.08	47.93	69.12	70.97
Low residential	2.17	27.65	29.82	41.46	43.63
Rural residential	33.41	9.20	42.61	13.80	47.21
Total	39.56	92.13	131.69	138.18	177.74
Fraction of sub-basin four (%)	18.23		60.69		81.91

precipitation and streamflow trends was undertaken. A 41 year (WY 1966–2006) record was established for both data sets. Regression analysis was conducted for the recorded data following the linear regression model of White and Greer (2006).The slope (*S*) of the regression lines was tested for significance using an analysis of variance (ANOVA), with significance defined as a p value of less than 0.01. Annual precipitation appears to decrease slightly (slope $= -0.48$; p value < 0.001) in the 41 year period, while annual runoff (slope $= 0.64$; p value < 0.001) shows a slight increase (Fig. 2). The estimated runoff coefficient remains relatively stable (slope $= -0.0016$; p value < 0.001). Further analysis is ongoing regarding urbanization and climate trends in the USCRW and other Southern California watersheds (not presented here).

The annual maximum, median, and minimum daily flow discharge were determined from the 41 year period record as well. The effluent discharges of two WRPs were deducted from these statistics during the period from 1975 to 2006 (when WRP discharge data are available). Regression analysis was conducted for the period 1975–2006 (Fig. 3). Annual minimum and medium flows decrease slightly from 1975 to 2006, while there is a slightly increasing tendency of maximum flow in the same period. Given the observed trends in the USCRW, we hypothesize that the observed increase in streamflow can be attributed primarily to anthropogenic influences (i.e., the addition of impervious surfaces, urban runoff from irrigation, etc.).

Average precipitation for the modeling (baseline) period (WY 1997–2006) was estimated at 419 mm, annual discharge at 59.8 mm and runoff partitioning (ratio) at 0.12. The modeling period contains several above normal precipitation years (WYs 1998 and 2005) as well as a few significantly drier years (WYs 1999, 2002, and 2004) (Fig. 4). The runoff ratio during the 10 year period varies from a low of 0.06 (WY 2003) to a high of 0.21 (WY 2005).

Model calibration and validation

Statistics including BIAS, *R*, RSR, and NSE associated with the four calibration scenarios were computed at the daily scale (calibration timestep) (Table 3). For all four model configurations (C1–C4), flows are somewhat underestimated by the model (negative bias ranging from −19.8% for C1 to −9.3% for C4). However, calculated values are in the satisfactory range based on published calibration guidance (Donigian 2002; Moriasi et al. 2007). In all four scenarios, simulated flows correlate well with the observed discharge ($R > 0.78$). Overall RSR ranges from 0.70 (C1) to 0.37 (C4). The NSE is somewhat low for C1 (0.52), but increases significantly for C3 (0.80) and C4 (0.87). Both the RSR and NSE were considered satisfactory for all scenarios according to the criteria presented by Moriasi et al. (2007). Scenario C1 (lumped) consistently produces the poorest statistics, while scenario C4 consistently provides the best statistics (Table 3). For the hybrid configurations (C2 and C3), the distributed precipitation

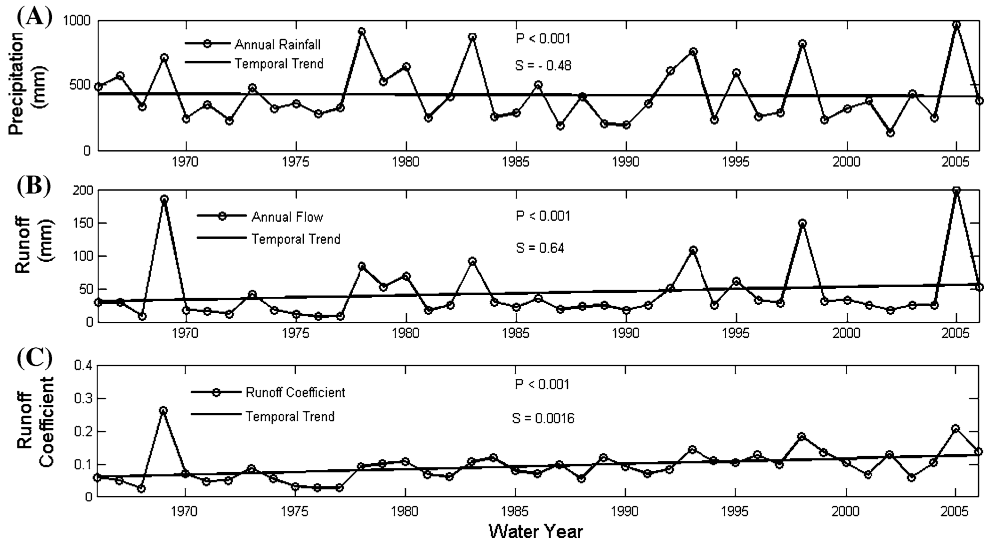

Fig. 2 Observed **a** precipitation, **b** runoff, and **c** runoff coefficient in the period from water year 1966–2006 of the study watershed. Linear regression lines are predicted from the 41 year data. *P* represents significance of regression coefficient; *S* denotes slope of the linear regression line

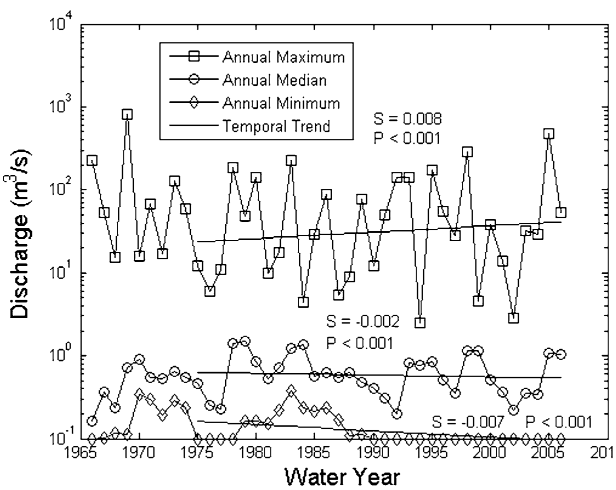

Fig. 3 Recorded annual maximum, median, and minimum discharge of the study watershed during the period 1966–2006. Linear regression lines are predicted from 1975–2006. *P* represents significance of regression coefficient; *S* denotes slope of the linear regression line

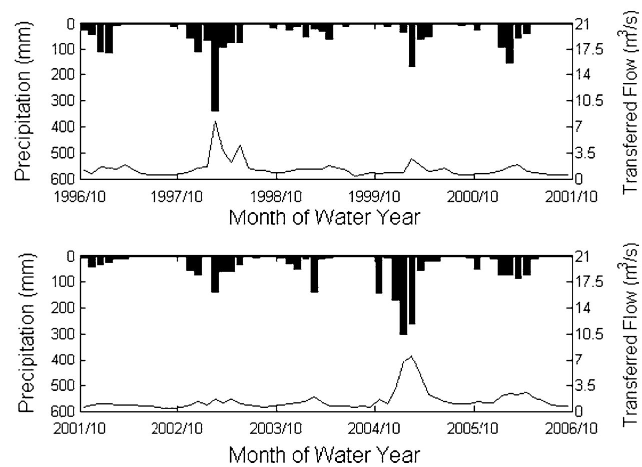

Fig. 4 Monthly time series of observed data for the modeling period. Precipitation is shown as a hyetograph (*inverted bars*) and monthly discharge (transformed flow) is shown as a *solid line*

input scenario with lumped parameters (C3) outperforms the distributed parameter scenario with lumped precipitation inputs (C2), highlighting the dependency of the model on spatial precipitation information and that the model appears more sensitive to variation in model inputs than model parameters.

Configuration C4 produced the best statistics and visual simulations and was selected as the model configuration for further analysis. Values for the final calibrated parameters, as well as model ranges (Duda et al. 2001) are listed in Table 4. Both calibration (WY 1999–2002) and validation (WY 2003–2006) results are evaluated for three time scales: annual, monthly, and daily. Statistics for all three time scales, as well as for dry and wet season flow (daily timestep) are presented in Table 5. Annual (Fig. 5a) and monthly (Fig. 5b) scatter plots illustrate that simulated flows match the observed discharge fairly well for both the calibration and validation periods. Overall, simulations during the calibration period show a slightly higher bias (−9.3% annual; −9.4% on the monthly) than during the validation period (0.4% annual; 0.5% monthly). However, bias values for both time scales and periods are considered in the "very good" range according to Moriasi et al. (2007). Furthermore, simulations during the calibration period result in much higher NSE values (0.96 annual and monthly) than during the validation period (0.52 annual; 0.72 monthly) at these time scales (Table 5).

Scatter plots generated at the daily timestep illustrate model performance in the wet season (Fig. 5c) and dry season (Fig. 5d) is acceptable but not as good as at the annual and monthly scales. Bias is noted at the low end of the model simulations. Performance during the wet season

Table 3 Calibration scenarios used to establish model design and corresponding statistics for model performance when compared with observed streamflow (USGS gage #11109000)

Scenarios			Calibration statistics			
Number	Precipitation input	Model parameters	% Bias	*R*	RSR	NSE
C1	Lumped	Lumped	−19.8	0.78	0.7	0.52
C2	Lumped	Distributed	−10.5	0.85	0.55	0.69
C3	Distributed	Lumped	−10.1	0.93	0.44	0.8
C4	Distributed	Distributed	−9.3	0.93	0.37	0.87

Calibration statistics include percent bias (% Bias), correlation coefficient (*R*), ratio of root mean squared error (RMSE) to standard deviation (RSR) and Nash–Sutcliffe Efficiency (NSE)

Table 4 Calibrated model parameters and feasible parameter ranges for both pervious and impervious land covers in the HSPF model

Parameters		Values		Unit
		Calibrated values	Model range[a]	
Previous cover				
FOREST	Fraction forest cover	0	0-1	None
LZSN	Lower zone nominal soil moisture storage	127–203	0.25–2,540	mm
INFILT	Index to infiltration capacity	1	0–2,540	mm/hr
LSUR	Length of overland flow	152	>0.3	m
SLSUR	Slope of overland flow plane	0.009–0.025	0–10	None
KVARY	Variable groundwater recession	0.59	>0	1/mm
AGWRC	Base groundwater recession	0.99	0–0.99	1/day
PETMAX	Temperature below which ET is reduced by half	4.4	0–8.8	°C
PETMIN	Temperature below which ET is set to zero	1.7	−1.1–4.4	°C
INFEXP	Exponent in infiltration equation	2	0–10	None
INFILD	Ratio of max/mean infiltration capacities	2	1–2	None
DEEPFR	Fraction of groundwater inflow to deep recharge	0.5–0.9	0–1	None
BASETP	Fraction of remaining ET from baseflow	0.02	0–1	None
AGWETP	Fraction of remaining ET from active groundwater	0	0–1	None
CEPSC	Interception storage capacity	2.54	0–254	mm
UZSN	Upper zone nominal soil moisture storage	51–89	0.25–2,540	mm
NSUR	Manning's n for overland flow	0.2	0–1	None
INTFW	Interflow inflow parameter	0.1	>0	None
IRC	Interflow recession parameter	0.5	0–0.99	1/day
LZETP	Lower zone ET parameter	0.7	0–1.5	None
Impervious cover				
LSUR	Length of overland flow	152	>0.3	m
SLSUR	Slope of overland flow plane	0.009–0.025	0–10	None
NSUR	Manning's n for overland flow	0.05	0–1	None
RETSC	Retention storage capacity	2.54	0–254	mm
PETMAX	Temperature below which ET is reduced by half	4.4	0–8.8	°C
PETMIN	Temperature below which ET is set to zero	1.7	−1.1–4.4	°C

[a] Ranges of model parameters obtained from Duda et al. (2001)

during the calibration period (NSE = 0.86) is very good, but poorer values are noted during the validation in the wet season (0.29). Dry season daily simulations result in NSE values of 0.72 for the calibration period and 0.48 for the validation period. Biases are increased (worse) during the calibration period for wet season daily flow; however, correlation and RSR values are better for both wet and dry season flows during the calibration period (Table 5).

Table 5 Statistics for model performance for both the calibration period (1999–2002) and validation period (2003–2006)

Scenarios	Categories	% Bias	R	RSR	NSE
Calibration (1999–2002)	Annual total flow	−9.3	0.99	0.21	0.96
	Monthly average flow	−9.4	0.99	0.20	0.96
	Daily flow	−9.3	0.93	0.36	0.87
	Daily wet season flow	−10.0	0.93	0.37	0.86
	Daily dry season flow	−1.9	0.85	0.53	0.72
Validation (2003–2006)	Annual total flow	0.4	0.76	0.70	0.52
	Monthly average flow	0.5	0.87	0.52	0.72
	Daily flow	0.3	0.69	0.82	0.32
	Daily wet season flow	−1.8	0.68	0.84	0.29
	Daily dry season flow	8.5	0.76	0.72	0.48

Results are presented for annual total flow, monthly average flow, daily flow, and wet and dry season daily simulations

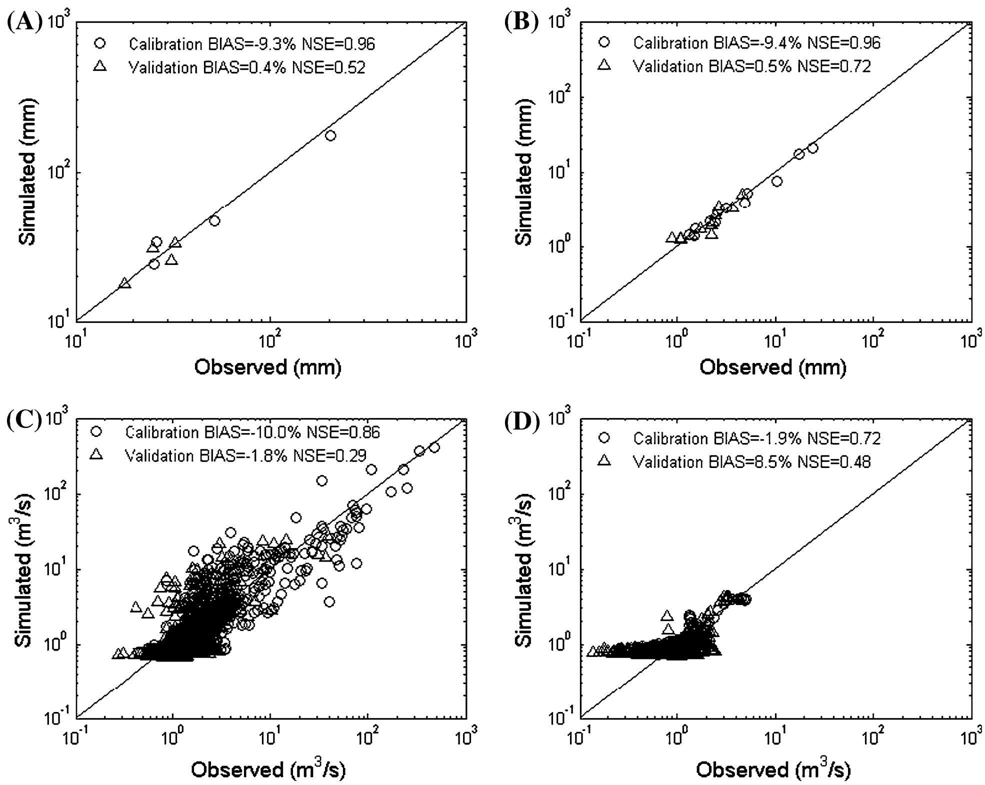

Fig. 5 Model calibration and validation results **a** observed versus simulated annual flow, **b** observed versus simulated monthly flow, **c** observed versus simulated daily flow during the wet season (October–May) and **d** observed versus simulated daily flow during the dry season (June–September)

Select hydrographs are also presented to allow visual inspection of model performance for a dry year (WY 2004, Fig. 6a) and a wet year (WY 2005, Fig. 6b). Transformed flow is used in plotting the hydrograph to allow for improved visualization of low flows. The transformation is formulated as follows (Hogue et al. 2006):

$$Q_{\text{trans}} = \frac{(Q_0 + 1)^{\lambda} - 1}{\lambda}, \quad \lambda = 0.3 \tag{5}$$

where Q_0 represents the raw flow vector, Q_{trans} represents the transformed flow vector, and λ is a constant coefficient ($\lambda = 0.3$ in this study). Simulated flows closely follow the observed flows (solid circles) for most of the years (Fig. 6). Peak flows are captured for the majority of events (except for the first small runoff event in the dry year). Simulation of recessions is not always satisfactory, especially during WY 2004. The model is not able to capture the falling limb of the hydrograph during the first big event in December of 2003, but does much better during the next large runoff event. Recessions are better simulated during the wet year and simulated flows match observations well for most of the entire water year. Timing is also fairly good in both years. In general, R, RSR, and NSE statistics (with the corresponding hydrographs) indicate that the model does

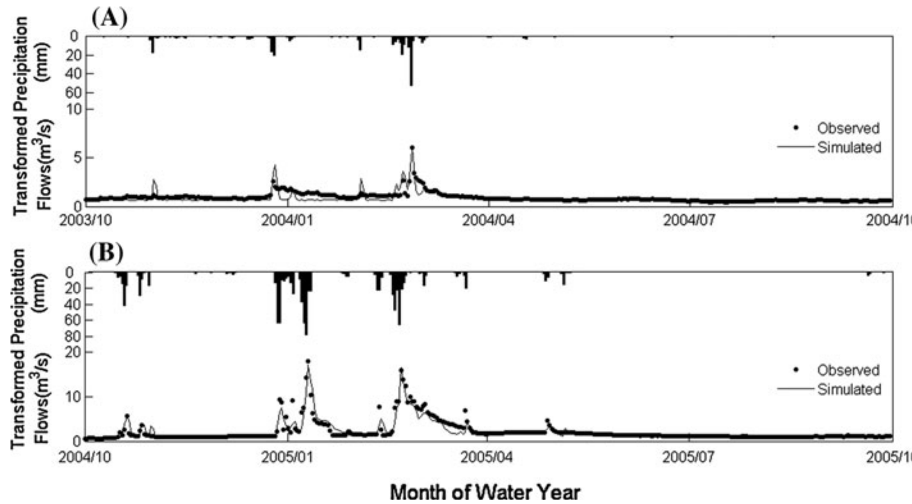

Fig. 6 Daily model simulation results for **a** a dry year (WY 2004), and **b** a wet year (WY 2005). Observed flow is shown as *closed circles* (•) while model simulation is shown as *solid line*. Precipitation for each year is also shown as an *inverted bar* above each hydrograph

consistently better during the calibration period (over the validation period). In addition, model performance is generally better during the wet season rather than the dry season.

Scenario modeling

Using the same model design and input (WY 1997–2006 and C4 model configuration), the USCRW model is reformulated by incorporating the proposed land use change for each respective development scenario (S1–S4). Flow regime changes corresponding to each scenario are simulated and interpreted on annual, monthly, and daily scales. Percent change is estimated relative to the baseline simulated values for the 1997–2006 period. Figure 7a shows the respective change in annual flow for each of the study years (WY 1997–2006). Average monthly changes are also shown for the wet months during the 10 year period (Fig. 7b) and for the dry months of the same period (Fig. 7c). The relative change of predicted total annual flows from the baseline (simulated under the current land cover scenario) varies annually within the 10 year simulation period, mostly due to the non-uniform distribution of precipitation (El Nino event in WY 1998; dry years in WY 1999 and WY 2002). For each year, the simulated annual total flow increases with increasing urbanization in the watershed, with the highest increase near 150% for S4 during El Nino year 1998. A consistent increase in predicted monthly average flows with increasing developed extent during the wet season (October–May) can also be identified (Fig. 7b). The largest change (around 180%) occurs during the wetter months of December and February and the lowest monthly changes occur in May (Fig. 7b). Dry season (Fig. 7c) changes in simulated monthly flows are significantly less in magnitude than during the wet season. Specifically, in July, the modeled monthly flow

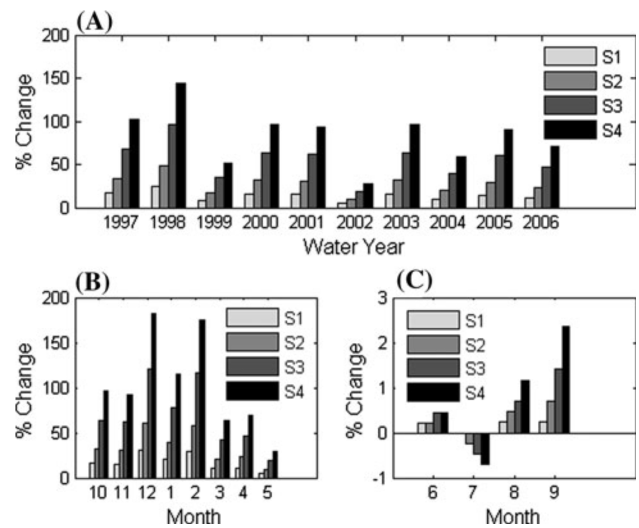

Fig. 7 Deviation (% change) from current streamflow conditions for **a** predicted annual total flow, **b** predicted monthly average flow during the wet season, and **c** predicted monthly average flow during the dry season for the four proposed development scenarios

decreases with increasing development. Average precipitation in July is near zero during the 10 year period. Observed streamflow during this month is primarily baseflow, with scenario results indicating that increasing urbanization decreases system baseflow (based on model simulations).

The selected 100 storms are evaluated with respect to changes in overall volume and peak flow (as compared to the baseline storm simulations). Daily flow exceedance curves for the simulation period (Fig. 8) illustrate that storms with extremely low volume and peak (>95%) and high volume and peak (<5%) for the four development scenarios show relatively little change compared to baseline conditions, while storms in the medium flow range show significant variations with increasing development in

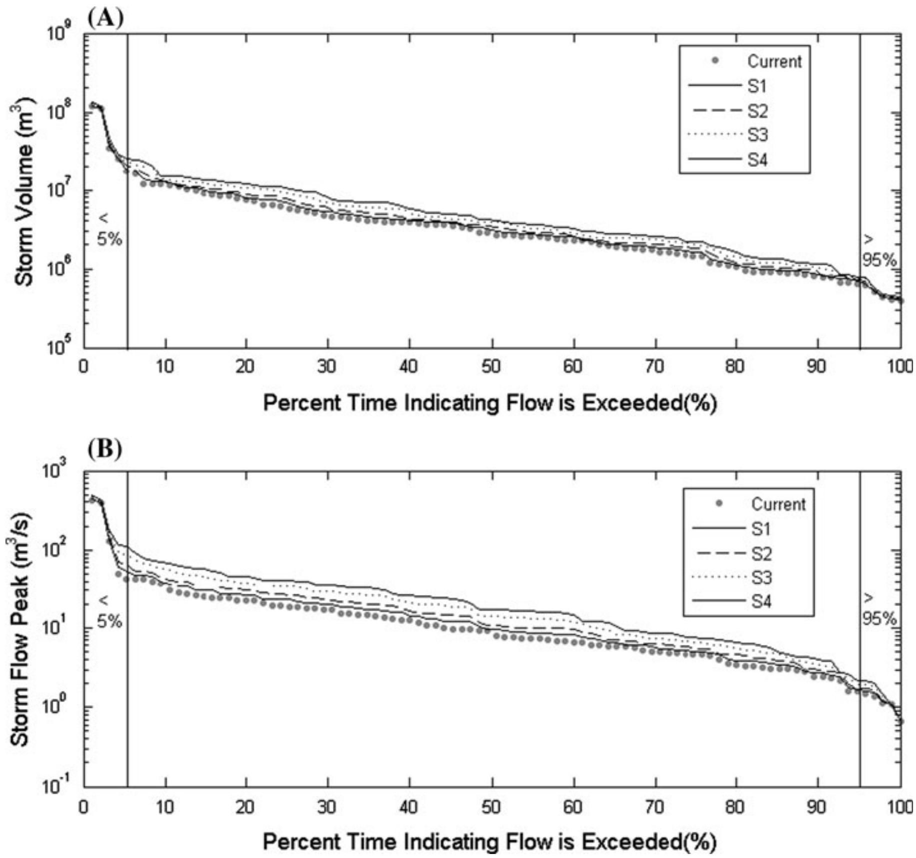

Fig. 8 Exceedance curve for **a** storm volume, and **b** storm flow peak simulated under current conditions and the four proposed development scenarios. *Vertical solid lines* represent 5 or 95% thresholds as designated

Table 6 Predicted volumes and peaks of storms for high (<5%), medium (5–95%), and low (>95%) magnitude flows, as well as relative change from current conditions for the proposed development scenarios (S1–S4)

Scenarios	High		Medium		Low	
	Value	% Change	Value	% Change	Value	% Change
Average volume (10^6 m^3)						
Current	61.04	–	3.96	–	0.47	–
S1	62.62	2.58	4.32	9.11	0.49	3.00
S2	64.22	5.20	4.68	18.23	0.50	6.06
S3	67.44	10.48	5.41	36.48	0.53	12.03
S4	70.65	15.73	6.13	54.77	0.56	18.05
Average peak (m^3/s)						
Current	207.70	–	12.06	–	1.15	–
S1	215.12	3.57	14.24	18.12	1.21	5.37
S2	222.65	7.20	16.46	36.46	1.27	10.74
S3	238.28	14.72	20.93	73.56	1.40	21.43
S4	254.08	22.33	25.46	111.12	1.52	32.27

both overall volume (Fig. 8a) and peak flow (Fig. 8b). In general, storm volume and peak increase with increasing development. As expected, the S4 simulations show the most significant increase. The average volume and peak of storms with various magnitudes (high, medium, and low) under the current condition and proposed scenarios are calculated (Table 6), as well as the percent change of average volume and peak simulated under projected development scenarios over the baseline condition (simulated under the current land cover). It is clear that the quantified results confirm the noted observations in the flow duration curves (Fig. 8). Specifically, in the extreme development scenario (S4), the average peak of medium storms is doubled (111.12% increase) and the average

Table 7 Predicted flow regimes for surface flow, baseflow, and recharge, as well as relative change from current conditions for the proposed development scenarios (S1–S4)

Scenarios	Runoff		Surface flow		Baseflow		Recharge	
	mm	% Change	mm	% Change	mm	% Change	mm	% Change
Dry season average								
Current	28.31	–	27.94	–	0.38	–	3.40	–
S1	28.35	0.13	27.98	0.16	0.37	−1.74	3.34	−1.74
S2	28.39	0.26	28.02	0.31	0.36	−3.31	3.28	−3.31
S3	28.46	0.53	28.11	0.62	0.35	−6.60	3.17	−6.60
S4	28.54	0.78	28.20	0.93	0.34	−9.94	3.06	−9.94
Wet season average								
Current	85.68	–	81.37	–	4.31	–	38.80	–
S1	106.06	23.78	101.82	25.13	4.24	−1.72	38.13	−1.72
S2	126.47	47.60	122.30	50.31	4.16	−3.40	37.48	−3.40
S3	167.03	94.95	163.02	100.34	4.02	−6.80	36.16	−6.80
S4	207.60	142.30	203.73	150.38	3.87	−10.19	34.84	−10.19

volume is increased by 54.77%. In comparison, urbanization appears to have more influence on storm peaks rather than overall storm volume.

In addition to total runoff, changes in specific flow regimes—baseflow, surface (overland and lateral) flow, and recharge (deep groundwater contribution)—are investigated for both wet and dry seasons (Table 7). The current flow (depth in mm) for each component—total runoff, surface flow, baseflow, and recharge—is noted for the current (baseline) conditions as well as each scenario. Percent change from the total simulated depth for each component is then calculated. In general, urbanization increases surface flow and generally decreases background baseflow values and recharge for both the wet and dry seasons. Baseflow and groundwater recharge estimates are both linearly related via the model parameter DEEPFR (discussed previously), thus the percent change of baseflow and groundwater recharge for specific development scenario show similar values for each scenario. For surface flows, an increase in average wet season flow varies from 25% (S1) to 150% (S4). In contrast, increase in average dry season flow only ranges from 0.16 to 0.93%. For baseflow, the magnitude of percent decrease in both seasons is comparable, with changes ranging from −1.74% (S1) to −9.94% (S4) for the dry season and from −1.72% (S1) to −10.19% (S4) for the wet season. The decrease in groundwater recharge is also comparable for both seasons, with losses up to 10% for the most extreme development (S4). The current proposed development plan results in nearly a 25% increase in daily wet season surface flows and an approximately 2% loss in baseflow and deeper subsurface flows (recharge). More extreme urbanization (S3 and S4) significantly impacts surfaces flows—increasing surface flow over 100% for extreme development cases.

Discussion and concluding remarks

The current study was undertaken to evaluate the long-term hydrologic impacts of adding additional impervious surfaces in a developing semi-arid watershed. The semi-distributed HSPF model was selected to simulate baseline or current conditions, future development scenarios (based on proposed development plans) were derived, and hydrologic response of various flow components was assessed for the planned development, as well as more extensive development. To focus on the discussion of the results, we review the objectives posed at the beginning of our analysis:

(1) Assess the applicability of the distributed HSPF model in semi-arid watersheds. The results presented in the current study demonstrate the applicability of the HSPF model for semi-arid watersheds. The model was calibrated with various spatial configurations of input and parameters values. Results show that HSPF performs fairly well in all calibration configurations; however, simulations with distributed precipitation input and parameter sets provide the best simulations. In addition, the calibration results at the daily time scale show a slight improvement over those previously reported in literature (Brun and Band 2000; Hayashi et al. 2004; Ackerman et al. 2005), with an overall bias of −9.3% and an NSE of 0.87 (calibration period). Percent bias and NSE values for simulated dry and wet season daily flows are −10 and −1.9%, and 0.86 and 0.72, respectively. On the annual and monthly scales, the HSPF has similar, or better, performance when compared to the daily time scale results. Visual inspection of simulated hydrographs further reveals that the model simulates the event peaks well in both dry and wet years and, in general, captures overall flow variability. Simulations during the validation period are acceptable, but generally not as good

as simulations during the calibration period. Correlation (*R*), RSR, and NSE values are degraded slightly for daily simulations during the validation period. However, biases are generally lower (better) in the validation period, except for dry season flows, where an increased bias of 8.5% is noted, compared to a bias of −1.9% for the dry season calibration period flows. In summary, the current analysis reveals that the HSPF model performs well for this semi-arid watershed at a range of time scales (daily to annual). Secondly, the model performs slightly better during wetter seasons and years than during drier periods.

(2) Predict changes in the hydrologic behavior (surface flow, infiltration, baseflow, storm response, etc.) to varying levels of potential urbanization. The distributed, validated HSPF model was used to evaluate the impacts of future urbanization on flow regimes in the USCRW. Results show that increasing development generally increases total annual runoff and wet season flows (total channel discharge). In comparison, the influence of development on total dry season flow is less certain due to the lack of rainfall during the dry months. In months with little to no precipitation, discharge was noted to decrease with increasing urbanization. Exceedance curves reveal that storms with medium discharge volumes (5–95% flow ranges) gradually increase as developed areas increase, while storms with extremely low volumes or high volumes appear less affected. As with previously published studies, urbanization increases surface (overland and lateral) flow (Wissmar et al. 2004; Murdock et al. 2004; Vicars-Groening and Williams 2007; Beighley et al. 2008; Im et al. 2009). Model simulations also indicate a decrease in baseflow response and a decrease in deep groundwater recharge in both the dry season and wet season. Under the proposed development plans (S1), both baseflow and recharge decrease by about 2% in sub-basin four. Given extreme development (S4), the decrease in baseflow and groundwater is estimated to be around 10%. Of note in the current study is the inability to account for potential increases in urban runoff during the dry season in HSPF model simulations. As previously discussed by Ackerman et al. (2005), heavily urbanized surfaces in semi-arid regions may see an increase in dry weather flows due to various anthropogenic activities that may use imported water which eventually ends up as channel flow during the dry season. An increase in dry weather flow will most likely be evidenced in the USCRW given increasing urbanization. Given the current HSPF model structure and lack of information on future imported water use, the estimates of baseflow response produced during the predictions of future urbanization (S1–S4) may have significant uncertainty. However, previous studies have noted general decreases in infiltration in urbanized regions (Finkenbine et al. 2000; Toran et al. 2009; Pandey et al. 2010), which will most likely be evidenced in the USCRW and is supported by the presented model predictions of declining recharge with increasing development. Although recharge validation is difficult, we feel fairly confident in the range of estimates produced from the model simulations. The HSPF model was well calibrated and showed improved results over previous studies. The model was calibrated primarily to total discharge, which includes both surface and baseflow components. Given the relative success of the model during low flows during inter-storm periods and relatively dry periods, we assert that both surface flow and baseflow processes are fairly well estimated under the current conditions. Hence, the residual component, recharge, is well estimated under current conditions given the success of the calibration and that predictions of changes in recharge for the proposed developments are therefore reasonable.

(3) Quantify the potential loss of subsurface water supply (recharge) given extensive basin development. Water supplies in Southern California are variable by water district and region, but in general include about half from imported water supplies (northern California, Colorado River, and Owens Valley) and the other half from local supplies (MWD 2005). Regional aquifers provide, on average, about 1.41 maf (1.74 Gm^3) groundwater per year (MWD 2005). Southern California's imported water supply may be extremely vulnerable to climate change effects. Observed declines in snowpack, along with projected declines in winter precipitation, could fundamentally disrupt the California water cycle (Hayhoe et al. 2004). There is evidence that some changes have already occurred, such as an earlier beginning date of spring snowmelt, an increase in winter runoff as a fraction of total runoff, and an increase in winter flooding frequency (Dettinger and Cayan 1995; Mote et al. 2005). The likelihood of dramatic declines in Colorado River flow is also significant and reservoir levels in the river have been significantly below capacity for several years (Christensen et al. 2004). California, which has been receiving more than its share of the Colorado River [~5.2 maf/year (6.41 Gm^3/year)], is under order by the Secretary of the Interior to return to regulated allocation levels of 4.4 maf/year (5.43 Gm^3/year) (Gelt 1997). Minor fluctuations in local groundwater supplies (i.e., potential loss of recharge to existing aquifer systems) will exacerbate already sensitive water supplies for the increasing population in Southern California.

The estimated changes in recharge for potential development in the USCRW, although relatively small in absolute numbers, equate to significant loss in recharge volume for the developing area. Sub-basin four in the USCRW, where the proposed development is focused, is approximately 217 km^2. A decline in recharge of 0.67 mm over the proposed basin (from aggregated model output) results in a volume loss of 0.145 Mm^3/year (primarily during the wet season). Given the current per capita water use in Southern California [$\sim$185 gal/day (0.7 m^3/day); MWD 2005], the recharge volume loss equates to a supply for around 600 people each year on average. For the extreme case (S4), the decrease in recharge of 3.96 mm across the sub-basin results in an estimated loss of 0.859 Mm^3/year, or enough water to supply approximately 3,400 people each year. Although the estimate of recharge loss from the S4 case is more extreme and includes significantly more uncertainty than estimates for the proposed level of development under S1, the case is presented to illustrate the potential impacts of cumulative, long-term development on watershed function and recharge loss.

In summary, this study is one of the first to address the impacts of cumulative development in a semi-arid watershed undergoing rapid and extensive development. Long-term, continuous simulations of potential urbanization are critical to further our understanding of basin-scale changes in flow regimes, especially in less-studied semi-arid watersheds. Seemingly minor decreases in recharge to local aquifers may result in significant volume losses when aggregated to the regional scale and considered over long time periods. Expanding populations in Southern California will be moving into regions where natural and extensive recharge has been occurring. Given the current uncertainty in precipitation and temperature trends, potential changes in existing and future water supplies need to be rigorously evaluated. Novel engineering and development strategies will be needed to prevent and/or mitigate alterations in watershed and native recharge processes due to continuing urbanization.

Acknowledgments This research was supported by funds from the University of California Water Resources Center (#WR-1007). The authors would like to acknowledge the Los Angeles County Department of Public Works and the Sanitation Districts of Los Angeles County for supplying precipitation data and discharge data from two wastewater reclamation plants, respectively. The authors also thank Rachel Stoll from the City of Santa Clarita and Hossein Nosseri (UCLA) for assistance with the regional development plan. The authors also appreciate the suggestions provided by Tom Jobes in model development.

References

Ackerman D, Schiff KC, Weisberg SB (2005) Evaluating HSPF in an arid, urbanized watershed. J Am Water Resour Assoc 41:477–486

Andriani GF, Walsh N (2009) An example of the effects of anthropogenic changes on natural environment in the Apulian karst (southern Italy). Envion Geol 58:313–325

Beighley RE, Dunne T, Melack JM (2008) Impacts of climate variability and land use alterations on frequency distributions of terrestrial runoff loading to coastal waters in Southern California. J Am Water Resour Assoc 44:62–74

Bhaduri B, Harbor JB, Engel B, Grove M (2000) Assessing watershed-scale, long-term hydrologic impacts of land use change using a GIS-NPS model. Environ Manage 26:643–658

Bicknell BR, Imhoff JC, Kittle JL Jr, Jobes TH, Donigian AS Jr (2001) Hydrological Simulation Program-FORTRAN (HSPF) User's manual for Version 12. US Environmental Protection Agency. National Exposure Research Laboratory, Athens, GA

Bledsoe BP, Watson CC (2001) Effects of urbanization on channel instability. J Am Water Resour Assoc 37:255–270

Brun SE, Band LE (2000) Simulating runoff behavior in an urbanizing watershed. Comput Environ Urban 24:5–22

Caraco DS (2000) Stormwater strategies for arid and semi-arid watersheds. In: Schueler TR, Holland HK (eds) The practice of watershed protection article 66. Center for Watershed Protection, Ellicott

Chen YD, Carsel RF, McCutcheon SC, Nutter WL (1998a) Stream temperature simulation of forested riparian areas I: watershed-scale model development. J Environ Eng-ASCE 124:304–315

Chen YD, McCutcheon SC, Norton DJ, Nutter WL (1998b) Stream temperature simulation of forested riparian areas II: model application. J Environ Eng-ASCE 124:316–328

Choi W, Deal BM (2008) Assessing hydrological impact of potential land use change through hydrological and land use change modeling for the Kishwaukee River Basin (USA). J Environ Manage 88:1119–1130

Christensen NS, Wood AW, Voisin N, Lettenmaier DP, Palmer RN (2004) Effects of climate change on the hydrology and water resources of the Colorado River basin. Climatic Change 62:337–363

Chung ES, Lee KS (2009) Prioritization of water management for sustainability using hydrologic simulation model and multicriteria decision making techniques. J Environ Manage 90:1502–1511

DePoto W, Gindi I, Schleikorn M (1991) Hydrology manual. Los Angeles County Department of Public Works, Hydraulics/Water Conservation Division, Alhambra, California, p 79

Dettinger MD, Cayan DR (1995) Large-scale atmospheric forcing of recent trends toward early snowmelt runoff in California. J Climate 8:606–623

Donigian ASJ Jr (2002) Watershed model calibration and validation: the HSPF experience. National TMDL Science and Policy, 2002 Specialty Conference, 30:1, Water Environmental Federation, Alexandria, VA

Duda P, Kittle J Jr, Gray M, Hummel P, Dusenbury R (2001) An interactive windows interface to HSPF (WinHSPF) User's manual, AQUA TERRA Consultants, Decatur

El-Kaddah DN, Carey AE (2004) Water quality modeling of the Cahaba River, Alabama. Environ Geol 45:323–338

Finkenbine J, Atwater J, Mavinic D (2000) Stream health after urbanization. J Am Water Resour Assoc 36(5):1149–1160

Gelt J (1997) Sharing Colorado River Water: history, public policy and the Colorado River compact. Water Resources Research Center Publication, University of Arizona, Tucson

Hayashi S, Murakami S, Watanabe M, Xu BH (2004) HSPF simulation of runoff and sediment loads in the Upper Changjiang River basin, China. J Environ Eng 130(7):801–815

Hayhoe K, Cayan D, Field CB, Frumhoff PC, Mauer EP, Miller NL, Moser SC, Schneider SH, Cahill KN, Cleland EE, Dale L, Drapek R, Hanemann RM, Kalkstein LS, Lenihen J, Lunch CK, Neilson RP, Sheridan SC, Verville JH (2004) Emission pathway, climate change, and impacts on California. PNAS 101:12422–12427

Hogue TS, Gupta HV, Sorooshian S (2006) A "user-friendly" approach to parameter estimation in hydrologic models. J Hydrol 320:202–217

Im S, Kim H, Kim C, Jang C (2009) Assessing the impacts of land user changes on watershed hydrology using MIKE SHE. Environ Geol 57:231–239

Keller AA, Zheng Y, Robinson TH (2004) Determining critical water quality conditions for inorganic nitrogen in dry, semi-urbanized watersheds. J Am Water Resour Assoc 40(3):721–735

Kim SM, Benham BL, Brannan KM, Zeckoski RW, Doherty J (2007) Comparison of hydrologic calibration of HSPF using automatic and manual methods. Water Resour Res 43(1):W01402. doi:10.1029/2006WR004883

Konrad CP, Booth DB, Burges SJ (2005) Effects of urban development in the Puget Lowland, Washington, on interannual streamflow patterns: consequences for channel form and streambed disturbance. Water Resour Res 41:W07009. doi:10.1029/2005WR004097

Land N (1999) Newhall ranch specific plan. Newhall Land, Valencia

Luo Y, Gao Q, Yang X (2007) Dynamic modeling of a chemical fate and transport in multimedia environments at watershed scale I: theoretical considerations and model implementation. J Environ Manage 83:44–55

Marcé R, Armengol J (2009) Modeling nutrient in-stream processes at the watershed scale using Nutrient Spiralling metrics. Hydrol Earth Syst Sc 13:953–967

McClintock K, Harbor J, Wilson T (1995) Assessing the hydrologic impact of land use change in wetland watershed: a case study from Northern Ohio, USA. In: McGregor D, Thompson D (eds) Geomorphology and land management in a changing environment. Wiley, New York, pp 107–119

Miller JR, Kochel RC (2010) Assessment of channel dynamics, in-stream structures and post-project channel adjustments in North Carolina and its implications to effective stream restoration. Environ Earth Sci 59:1681–1692

Moriasi DN, Arnold JG, Van Liew MW, Bingner RL, Harmel RD, Veith TL (2007) Model evaluation guildelines for systematic quantification of accuracy in watershed simulations. T ASABE 50(3):885–900

Mote PW, Hamlet AF, Clark MP, Lettenmaier DP (2005) Declining mountain snowpack in western North America. B Am Meteorol Soc 86:39–49

Murdock J, Roelke D, Gelwcik F (2004) Interactions between flow, periphyton, and nutrients in a heavily impacted urban stream: implications for stream restoration effectiveness. Ecol Eng 22:197–207

MWD (Metropolitan Water District) (2005) Metropolitan water District urban water management plan. Metropolitan Water District of Southern California, CA

NOAA-CSC (National Oceanographic Atmospheric Administration-Coastal Services Center) (2003) Southern California 2000-Era land cover/land use, LANDSAT-TM, 30 m. NOAA-CSC, Charleston

Ourso RT, Frenzel SA (2003) Identification of linear and threshold responses in streams along a gradient of urbanization in Anchorage, Alaska. Hydrobiologia 501:117–131

Pandey VP, Chapagain SK, Kazama F (2010) Evaluation of groundwater environment of Kathmandu Valley. Environ Earth Sci 60:1329–1342

Philips JR (1957) The theory of infiltration: the infiltration equation and its solution. Soil Sci 83:345–375

Quan RS, Liu M, Lu M, Zhang LJ, Wang JJ, Xu SY (2010) Waterlogging risk assessment based on land use/cover change: a case study in Pudong New Area, Shanghai. Environ Earth Sci. doi:10.1007/s12665-009-0431-8

Refsgaard JC, Knudsen J (1996) Operational validation and inter-comparison of different types of hydrological models. Water Resour Res 32(7):2189–2202

Tiefenthaler L, Schiff K, Leecaster M (2001) Temporal variability patterns of stormwater concentrations in urban stormwater runoff. In: Weisberg SB, Hallock D (eds) Southern California Coastal water Research Project annual report 2000. Southern California Coastal Water Research Project, Westminster, pp 28–44

Tong STY, Chen W (2002) Modeling the relationship between land use and surface water quality. J Environ Manage 66:377–393

Toran L, Gross K, Yang Y (2009) Effects of restricted recharge in an urban karst system. Environ Geol 58:131–139

USEPA (US Environmental Protection Agency) (2004) BASINS 3.1: better assessment science integrating point and non-point sources 3.1. USEPA, Washington

Vicars-Groening J, Williams HF (2007) Impact of urbanization on storm response of White Rock Creek, Dallas, TX. Environ Geol 51:1263–1269

White MD, Greer KA (2006) The effects of watershed urbanization on the stream hydrology and riparian vegetation of Los Penasquitos Creek, California. Landscape Urban Plan 74:125–138

Wissmar RC, Timm RK, Logsdon MG (2004) Effects of changing forest and impervious land covers on discharge characteristics of watersheds. Environ Manage 34:91–98